Journal of Medicinal Chemistry

Brief Article

pubs.acs.org/jmc

Affinity-Guided Design of Caveolin-1 Ligands for Deoligomerization

Amanda J. H. Gilliam,[†] Joshua N. Smith,[‡] Dylan Flather,[‡] Kevin M. Johnston,[†] Andrew M. Gansmiller,[†] Dmitry A. Fishman,[†] Joshua M. Edgar,[†] Mark Balk,[†,§] Sudipta Majumdar,[†] and Gregory A. Weiss*[,†,‡]

[†]Department of Chemistry, and [‡]Department of Molecular Biology and Biochemistry, University of California, Irvine, California 92697-2025, United States

Supporting Information

ABSTRACT: Caveolin-1 is a target for academic and pharmaceutical research due to its many cellular roles and associated diseases. We report peptide WL47 (**1**), a small, high-affinity, selective disrupter of caveolin-1 oligomers. Developed and optimized through screening and analysis of synthetic peptide libraries, ligand **1** has 7500-fold improved affinity compared to its T20 parent ligand and an 80% decrease in sequence length. Ligand **1** will permit targeted study of caveolin-1 function.

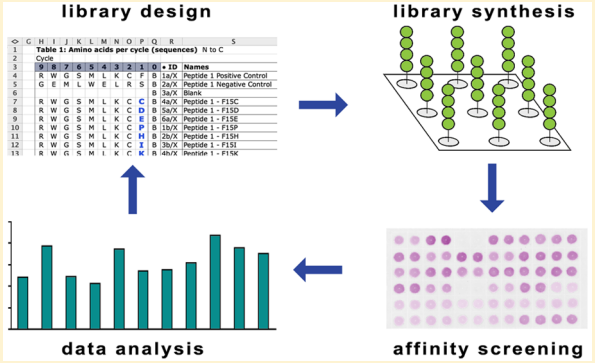

INTRODUCTION

The family of caveolin membrane proteins contribute to the cell's structural, signaling, and transportation processes. With such diverse roles, caveolins are also associated with myriad diseases, including cancer, cardiovascular disease, muscular dystrophies, atherosclerosis, diabetes, Alzheimer's disease, and HIV.[1−5] Although the caveolins represent excellent candidate targets for drug discovery, progress has been hampered by a lack of tools to probe and control caveolin structure and functions with specificity and precision. Caveolins are typically studied in cells and organisms through ablation via knockouts, mutagenesis, deletions, or nonspecific cholesterol depletion using compounds.[6−11] Here we report a molecular tool to disrupt oligomerization of the most widely distributed and commonly studied caveolin, caveolin-1 (CAV). This CAV ligand also provides a potential lead compound for a new class of therapeutics.

As a monotonic membrane protein, CAV, a 22 kDa protein, penetrates only one leaflet of the lipid bilayer, and the N- and C-termini remain on the cytoplasmic side.[12] Multiple copies of CAV oligomerize to form high molecular weight complexes that bend the membrane inward to form invaginations, termed "caveolae", of 50−100 nm in diameter.[13,14] The cholesterol- and sphingolipid-rich membrane of these caveolae regions is a subtype of lipid raft.[15] These invaginations can mediate endocytosis in a manner similar to clathrin-coated pits. CAV's binding partners include cAMP-dependent protein kinase A (PKA), endothelial nitric oxide synthase (eNOS), insulin receptors, and the HIV coat protein gp41.[16,17] CAV modulates signaling pathways by binding and sequestering enzymes and receptors engaged in cell signaling. The complex with oligomeric CAV can stabilize such enzymes or receptors in their active or inactive conformations. CAV also mediates cholesterol trafficking by binding and transporting cholesterol. The oligomeric state of CAV also influences early cellular response to mechanical stress.[18,19]

Previous research in the Weiss laboratory used the known interaction between CAV and gp41 (**2**) as a starting point for generating a ligand for CAV.[20] The FDA-approved drug T20 (**3**), a 36 amino acid peptide derived from gp41, blocks HIV viral fusion with $CD4^+$ T-cells.[21,22]

The T20 sequence was mutated extensively in a phage-displayed library for screening and selections targeting CAV residues (1−104), a truncated form of CAV that can be expressed solubly in bacteria in contrast to wild-type CAV. From this library, 36-mer sequence **4** was isolated with dissociation constants (K_D) for CAV(1−104) of >155 nM. This phage-based, molecular evolution represented a 1000-fold improvement in K_D relative to T20.[20]

We have undertaken further design refinement of this T20-derived CAV ligand, **4**.[20] Iterative cycles of synthesis and assay guided the design to yield an 80% reduction in length with 7.5-fold higher affinity (Figure 1). By synthesizing and screening carefully designed peptide library arrays, we also identified key residues, minimized ligand size, and optimized the sequence (Figures 2−4). We report that this ligand, **1**, has high selectivity and affinity for its target (Figures 5 and 6) and can disrupt CAV oligomers (Figure 7).

Received: October 1, 2015
Published: March 24, 2016

DOI: 10.1021/acs.jmedchem.5b01536
J. Med. Chem. 2016, 59, 4019−4025

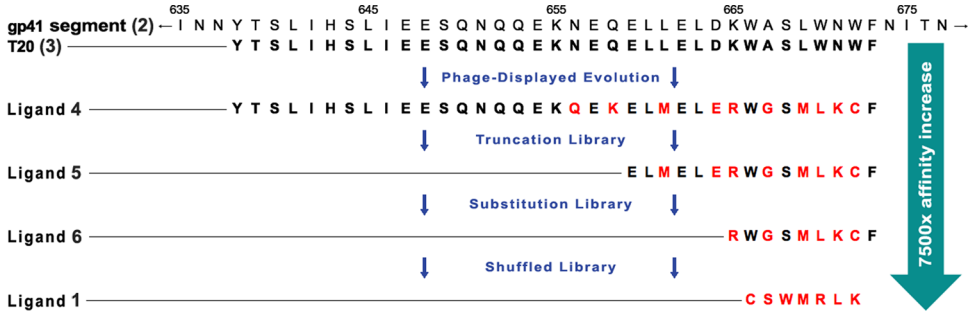

Figure 1. Evolution of CAV ligands. Sequence alignment showing the progression of peptide ligands from the gp41 segment sequence (**2**) to T20 (**3**) to ligands **4**, **5**, and **6** and ultimately to ligand **1**, which binds CAV(1−104) with 7500-fold higher affinity despite an 80% decrease in length compared to **3**. Residues mutated from **3** are colored red. Numbers above **2** indicate the residue numbers from the original protein.

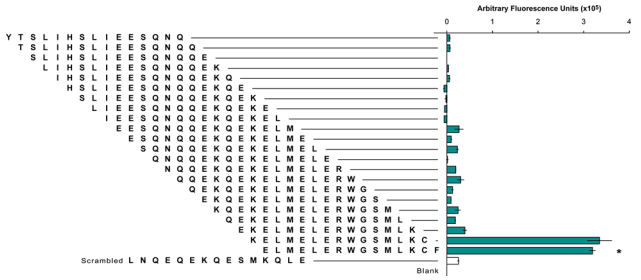

Figure 2. Initial identification of CAV interacting region. The sequence of ligand **4** was truncated to generate 22 unique peptide 15-mer sequences. Only two truncation sequences, consisting of residues 21−35 and residues 22−36, respectively, bound CAV(1−104) more than 2-fold above the level of the negative control. The negative control was a scrambled sequence of the randomly selected 11th truncation. An additional, blank negative control had only a linker region. The sequence corresponding to residues 22−36 (indicated by asterisk) was chosen as the template for subsequent libraries and designated ligand **5**.

RESULTS AND DISCUSSION

Development of ligand **1** proceeded in three stages (Figure 1). First, regions of the starting ligand **4** contributing to CAV binding were identified. Second, this functional region was trimmed though mutagenesis and screening to eliminate nonessential residues. Third, the remaining key residues were shuffled to identify the most promising arrangement.

First, truncation libraries identified key regions of the starting T20-derived, ligand **4** (Figure 2). Such information could reduce the length of the ligand required for CAV binding. The 22 possible 15-mer sequences within the 36-mer peptide **4** were synthesized and screened as C-terminal adducts to cellulose. This technique, termed SPOT synthesis, allows rapid synthesis and screening of peptides in a positionally addressable array.[23] The concentration of peptide in each SPOT can vary due to differences in amino acid coupling efficiency during synthesis. Nonetheless, investigation of the level of variation in peptide concentration between SPOTs confirmed that such variation is small compared to the observed differences in binding (Table S1 in Supporting Information). This method can thus provide reliable comparisons of binding affinity between peptides on the same array.[24,25]

SPOT synthesis provided a dependable method to guide the development of ligand **1**. CAV(1−104) bearing a fluorescent rhodamine tag was incubated with the peptide array, and the degree of fluorescence measured for each library member revealed its relative binding affinity. This experiment identified the C-terminal region of ligand **4** as contributing at least 98% of the affinity for CAV(1−104) (Figure 2). Thus, eliminating the nonessential region at the N-terminus reduced ligand size from a 36- to a 15-mer peptide, ligand **5**.

Additional trimming and mutagenesis next honed the CAV ligand. With the 15-mer peptide **5** as a template, the next library featured similar and dissimilar substitutions at each position. This approach defines any side chain contributions to binding. Screening every member of a chemically synthesized library circumvents the problem of survivorship bias, which can be inherent to molecular evolution approaches. By inclusion of every library member in the data set, the results from ligands with poor apparent binding affinity can still contribute to a deeper understanding of the functionalities that control CAV ligand affinity.

This substitution library uncovered peptides with clear preferences for amino acid side chains in specific positions. Library members with Lys or His substituting Arg7 retained apparent binding affinity to CAV(1−104), but substitution with the neutral side chains of Gln or Ala at this site generated a peptide with reduced apparent affinity for CAV(1−104). Substitution of Lys13 had similar but more drastic changes, with Arg substitution retaining complete potency and His, Gln, or Ala substitution abolishing binding. Taken together, these data demonstrate the importance of the two positively charged Lys and Arg side chains (Figure 3a).

Furthermore, the three negatively charged Glu residues clustered at the N-terminus of ligand **5** demonstrated no benefit for ligand binding. For example, substitution at Glu1, Glu4, or Glu6 with Ala or Gln resulted in peptides with equal or slightly better apparent binding affinity, while substitution with Lys at these sites moderately improved binding (Figure 3b). Removing six residues at the N-terminus, including these three negatively charged Glu, produced a 9-mer peptide with an approximately 3-fold increase in apparent binding affinity. Other truncations were less successful. For example, further truncation of the N-terminus eliminated the positively charged Arg7 and produced a sharp reduction in binding (Figure 3c). This result reemphasizes the importance of the positively charged side chains. In summary, this SPOT-synthesized library truncated six residues to yield a 9-mer peptide, ligand **6**, with increased apparent affinity for CAV(1−104).

Reduced ligand length made it feasible to synthesize a library with more substitutions. Each position of ligand **6** was systematically varied to examine side chain requirements for binding. A library was synthesized by SPOT synthesis to include 19 amino acid substitutions for each of the nine positions in ligand **6**, yielding 171 unique sequences each

DOI: 10.1021/acs.jmedchem.5b01536
J. Med. Chem. 2016, 59, 4019−4025

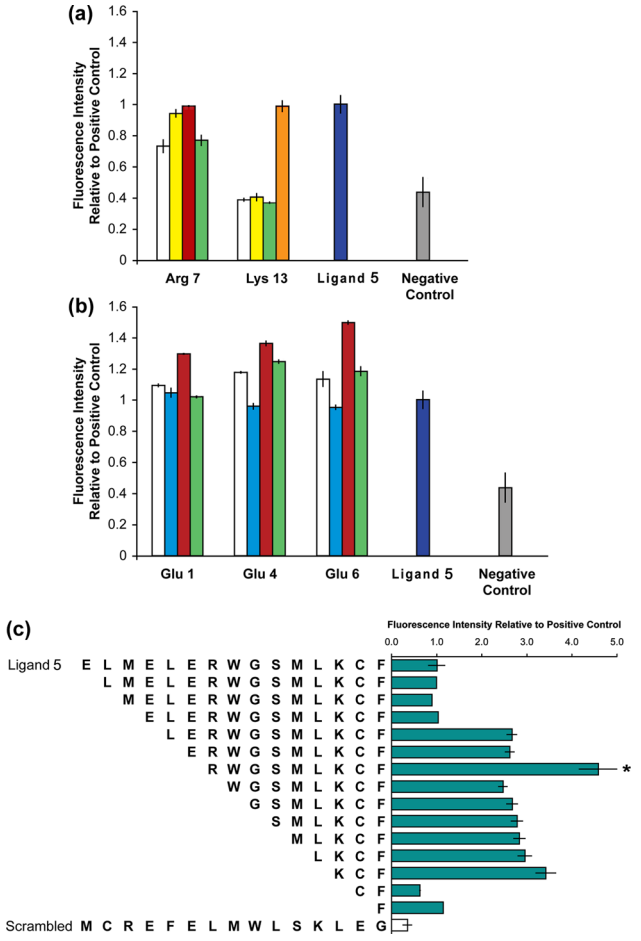

Figure 3. Identification of key residues and removal of detrimental amino acids. (a) In the library of similar and dissimilar substitutions of amino acids in ligand **5**, at Arg7, ligand binding was retained for Lys and His substituents but was reduced by neutral Gln or Ala substituents. At Lys13, ligand binding was eliminated for all substituents except Arg. We conclude that both these residues contribute to binding primarily via positive charge. (b) When Glu1 is substituted, ligand binding was retained for substitution with the negatively charged Asp or the neutral Gln and Ala. When Glu4 and Glu6 are substituted, ligand binding was slightly improved for substitution with the Gln and Ala and was slightly reduced for substitution with Asp. Positively charged Lys moderately improved binding in all cases. Data, therefore, suggest that Glu is not optimal in any of the three sites. (c) Truncation of the six N-terminal residues, which included all three Glu, without removing any of the positively charged residues yielded a peptide (indicated by asterisk) designated ligand **6** that became the template for subsequent library design. All libraries include a scrambled ligand **5** sequence as a negative control.

bearing a single substitution, along with unsubstituted ligand **6** as a positive control. The most striking data from this library were decreased apparent binding affinity for nearly all substitutions for Cys14 (ligand **5** numbering, Figure S1a). This observation strongly suggests that ligand binding requires dimerization through a disulfide bond. Notably, Leu and Tyr substitutions of Cys14 were well tolerated; these positions could accommodate hydrophobic residues capable of forming noncovalent interactions that most likely induce ligand dimerization as well. Dimerization by disulfide bond was investigated further using peptides in solution (below).

The initial library data also identified residues not contributing significantly to ligand function (Figure S1b). Such information guided trimming of the peptide to its minimum length. Up to this point, unnecessary residues were easily removed by simple truncation. For example, Phe15 could be clipped from the C-terminus and leave essential residues untouched, a desirable change to potentially remove nonspecific binding.[26] However, direct removal of an internal residue such as Gly9 could disrupt spacing of amino acids.

Since evolution and library screening identified key side chain functionalities, a library was synthesized omitting Gly and Phe and shuffling the remaining residues using the GenScript scrambled library peptide library design tool.[27] A total of 17 shuffled sequences were randomly chosen for synthesis and screening (sequences in Table S2). As expected, simple removal of Gly and Phe without otherwise altering the sequence (ligand **6**(ΔGF)) resulted in a roughly 25% reduction in apparent binding affinity relative to ligand **6**. However, a sequence seven residues in length and with 2.6-fold increased binding affinity relative to ligand **6** was isolated from this library (Figure 4). This sequence, ligand **1**, was chosen as the lead compound for further analysis.

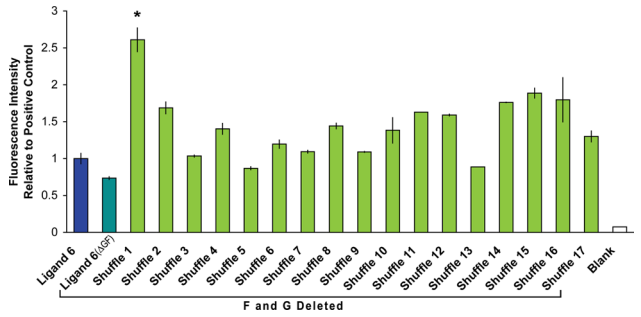

Figure 4. Unnecessary residues removed and sequences shuffled. Direct removal of Gly9 and Phe15 from ligand **6** sequence to create ligand **6**(ΔGF) decreased binding. When the sequence lacking Gly and Phe is shuffled, however, many library members demonstrate retained or improved binding affinity relative to ligand **6**. The 7-mer shuffled sequence (asterisk) with the highest apparent binding affinity was renamed ligand **1** and used in subsequent studies.

A parallel SPOT screening assay next examined the specificity of ligand **1** for CAV. In this assay, rhodamine-labeled CAV(1−104) and three other rhodamine-labeled proteins chosen for their solubility, ubiquity, and known nonspecific binding properties were each incubated with identical SPOT arrays on which ligands **5**, **6**, and **1** had been synthesized along with blank SPOTs bearing only the dual β-Ala linker. The sheets were washed, blocked, and then their fluorescence was quantified as described above. Ligand **1** binding to CAV(1−104) was significantly stronger than its binding to the other proteins. Furthermore, ligand **6** shows an increase in CAV(1−104) binding relative to ligand **5**, and ligand **1** has increased binding relative to ligand **6**, confirming that the iterative process effectively creates ligands with enhanced target binding. Conversely, little change in binding to control proteins is seen across the three ligand generations, affirming that specific rather than nonspecific binding has been enhanced during ligand evolution (Figure 5).

The K_D of the binding interaction between CAV(1−104) and ligand **1** was determined using the measured increase in fluorescence anisotropy of mantyl-**1** upon binding to its target. Slightly smaller than Phe, the *N*-methylanthranilyl "mantyl" fluorophore offers minimal bulk to reduce potential binding

DOI: 10.1021/acs.jmedchem.5b01536
J. Med. Chem. 2016, 59, 4019−4025

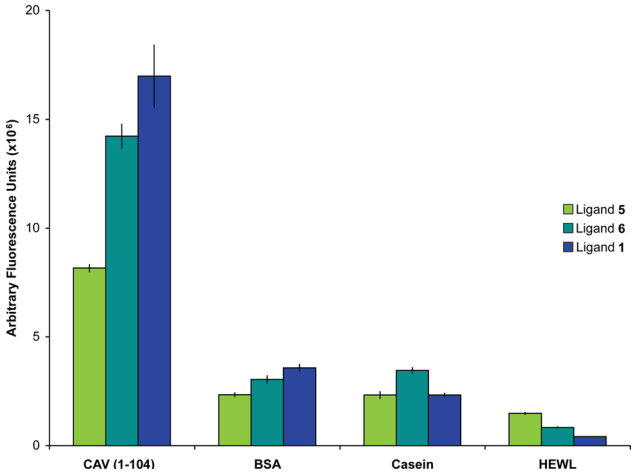

Figure 5. Demonstration of selectivity. CAV(1−104) and several control proteins were labeled with rhodamine and screened against duplicate SPOT sheets containing ligands **5**, **6**, and **1** to demonstrate selectivity of the ligand. Bovine serum albumin (BSA), casein, and hen egg white lysozyme (HEWL) all bound ligand **1** with reduced apparent affinity relative to CAV(1−104) as measured by fluorescence. Blank SPOTs containing only the double β-Ala linker were included as negative controls, and these baseline signals were subtracted from the corresponding signal for ligands **5**, **6**, and **1** SPOTs on each sheet.

disruption.[28] This fluorophore was installed to create mantyl-**1**. Varying concentrations of CAV(1−104) ranging from 0 to 586 nM were incubated with 12 nM mantyl-**1** dimers. Data were fit to the following equation described previously:[29]

$$\frac{[LR]}{[L]} = \frac{([R] + [L] + K_D) - (([R] + [L] + K_D)^2 + 4[R][L])^{0.5}}{2[L]} \quad (1)$$

where [L] is the total concentration of mantyl-**1** dimer, [R] is the total concentration of CAV(1−104), and [LR] is the concentration of Mantyl-**1** dimer bound to CAV(1−104). Equation 1 does not ignore binding site depletion, which is crucial for obtaining an accurate model when the ligand concentration is within an order of magnitude of the K_D value.[29] By this method, a K_D of roughly 23 nM was determined; the binding affinity ranged from 44 to 3 nM with 95% confidence (Figure 6a). A Hill plot of the data yields a Hill coefficient (n_H) of 1.97. This coefficient indicates virtually complete positive cooperativity in a two-site binding model; binding of one ligand **1** sequence (first half of dimer) to the first binding site induces the immediate binding of second ligand **1** sequence (second half of dimer) to the second site.[30] In essence, both binding sites become occupied simultaneously. This observation supports the decision to perform K_D calculations with dimerized ligand **1** treated as a single ligand (Figure 6b).

Demonstrating ligand **1** activity requires in vitro CAV. A full-length, soluble variant of CAV (CAV(FLV)) that spontaneously oligomerizes to form CAV nanoparticles with diameters consistent with those in caveolae (J.N.S. and G.A.W., unpublished results) was used to examine deoligomerization by ligand **1**. Ligand **1** effectively disrupts these nanoparticles. In the presence of a reducing agent, incubation of CAV(FLV) with ligand **1** does not disrupt oligomerization, which is consistent with the requirement for ligand **1** to dimerize through a disulfide bond (Figure 7a). Deoligomerization by ligand **1** was also dose-dependent (Figure 7b).

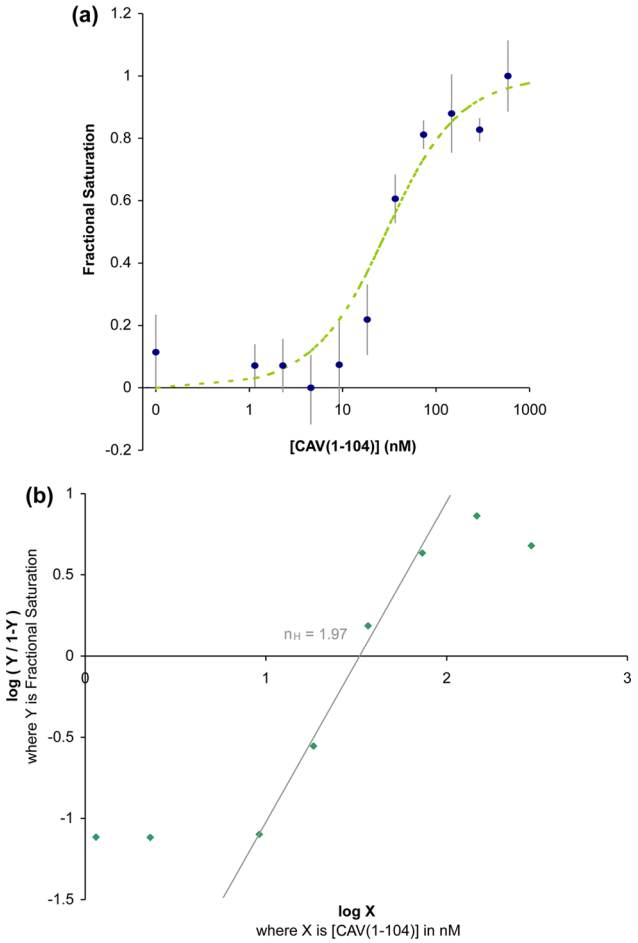

Figure 6. Binding affinity and cooperativity. (a) Fluorescence anisotropy was measured for the mantyl-**1** (as a dimer) incubated with the indicated concentrations of CAV(1−104). Using eq 1, a best fit binding curve was fit to the raw data using a weighted method of least-squares and assuming each ligand **1** dimer functions as a single ligand. The K_D for this ligand was calculated as 23 nM. (b) A Hill plot yields a Hill coefficient (n_H) of 1.97. This is the slope of the linear region of the plot as it crosses the x-axis (R^2 = 0.992).

Oligomerization and deoligomerization are essential to CAV activity and caveolae formation.[18,19] The overlapping nature of the oligomerization and scaffolding domains suggests the regulatory function of CAV relies upon its oligomeric state, as shown previously through oligomer complementation.[31]

Analysis of ligand **1** as a dimerized ligand allows for more critical analysis of previous work and suggests that both sites of a two-site system must be filled for deoligomerization of CAV. For example, isothermal calorimetry (ITC) data from Majumdar et al. suggested a two-site binding model with negative cooperativity between ligand **4** and CAV.[20] For dimeric ligand **1**, interaction with the first binding site could enforce binding to the second binding site via a proximity effect, overcoming the previously observed negative cooperativity. On the basis of the large positive ΔS_2, binding to the second site was proposed to be entropically driven, likely by the "disruption of caveolin oligomers upon binding".[20] This matches our observation that deoligomerization only occurs when ligand **1** is dimerized such that the second binding site is filled. Thus, data from dimeric **1** reinforce and clarify conclusions obtained with ligand **4**.

DOI: 10.1021/acs.jmedchem.5b01536
J. Med. Chem. 2016, 59, 4019−4025

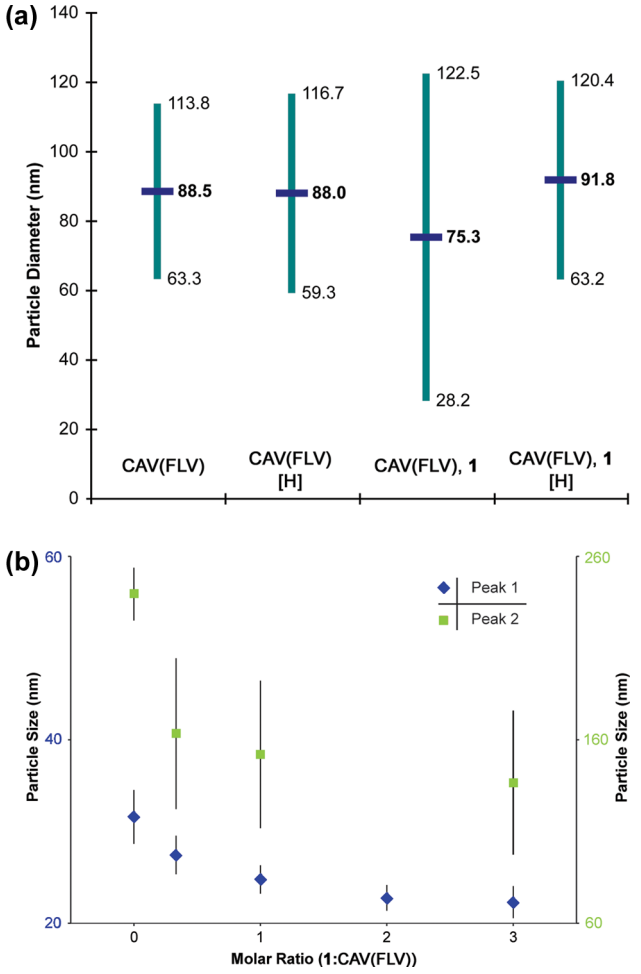

Figure 7. Disruption of oligomers. (a) CAV(FLV) spontaneously forms oligomers, measured here by dynamic light scattering (DLS). In this experiment, these oligomers had an apparent average diameter near 90 nm with polydispersity (indicated in teal) corresponding to approximately a 55 nm range. Incubating these oligomers with ligand **1** resulted in reduced average diameter and increased polydispersity, which are the expected outcomes of deoligomerization. With the disulfide dimerization of the ligand disrupted by reducing conditions by [H], no deoligomerization effect was observed. (b) In a separate DLS experiment, CAV(FLV) oligomeric peaks for 32 nm (blue, left axis) and 240 nm diameter particles (green, right axis) each showed a dose-dependent reduction in diameter, associated with deoligomerization, when incubated with ligand **1**.

As the first validated synthetic ligand for CAV, ligand **1** contributes to the ongoing debate over the existence and identity of a specific CAV binding motif. A characteristic binding motif with spaced aromatic amino acids, identified from phage display libraries selected against CAV residues 1−101, has been proposed.[32] In subsequent research, many CAV binding proteins included similar sequences.[1] However, comparing such aromatic spacing in CAV binding proteins with incidence in the proteome reveals no statistical enrichment of the motif in CAV binding proteins.[33] The ligand **1** sequence does not have multiple aromatic residues and thus does not conform to the canonical CAV binding motif; whether this motif mediates CAV binding for some proteins or not, it is clearly not the only way to target CAV. Since CAV has many binding partners, the interaction between CAV binding motifs and the CAV scaffolding domain likely evolved as a collection of low affinity interactions to allow CAV interactions with multiple partners.[34] Notably, the initial phage display process produced a higher affinity binder with fewer aromatic residues, and subsequent optimization produced ligand **1**, which diverges entirely from the CAV binding motif.

CONCLUSION

The CAV ligand (**1**) is 80% smaller in length and has 7500-fold greater affinity than the original T20 parent sequence (**3**) while also demonstrating selectivity and deoligomerization activity. This ligand was developed through a generalizable peptide ligand optimization process involving iterative library design, synthesis, and screening. Ligand **1** provides a new tool for research that will allow investigators to probe the functions of CAV with unprecedented selectivity, and its application to live cell assays is currently underway.

Beyond providing a new tool, the development of ligand **1** demonstrates the ways in which small molecule medicinal chemistry principles can be successfully applied to the creation of peptide ligands. Recent novel peptide ligands have been derived exclusively from direct mimicry of existing sequences from known proteins.[35,36] Conversely, the creation of novel small molecule drugs has involved greater experimentation and rational design. The application of these varied strategies ultimately allowed us to progress from our lead compound **1**, which had an interaction with CAV too weak to be successfully measured by ITC, to a ligand sequence that binds CAV with a K_D of 23 nM.

MATERIALS AND METHODS

Fmoc-protected amino acids for peptide synthesis were obtained from multiple suppliers, including NovaBiochem, ChemImpex, Anaspec, and Aroz Tech. All other reagents and materials were obtained through Sigma-Aldrich or Fisher Scientific unless otherwise noted. Peptides were synthesized as C-terminal adducts to cellulose as described in Hilpert et al.[37] or by standard solid phase peptide synthesis as detailed in Supporting Information.

ASSOCIATED CONTENT

Supporting Information

The Supporting Information is available free of charge on the ACS Publications website at DOI: 10.1021/acs.jmedchem.5b01536.

Expanded experimental methods; variation in peptide concentration between SPOTs; sequences for peptide library corresponding to Figure 4; further SPOT synthesis data analysis; HPLC traces demonstrating **1** and mantyl-**1** purity; additional references (PDF)

AUTHOR INFORMATION

Corresponding Author

*E-mail: gweiss@uci.edu. Phone: 001-949-824-5566.

Present Address

§M.B.: Eindhoven University of Technology, Den Dolech 2, 5612AZ Eindhoven, The Netherlands.

Notes

The authors declare no competing financial interest.

ACKNOWLEDGMENTS

We thank the National Institute of General Medical Sciences of the NIH for support (Grants R01GM078528-01, 1R0GM100700-01) and Vertex Pharmaceuticals for a graduate

DOI: 10.1021/acs.jmedchem.5b01536
J. Med. Chem. 2016, 59, 4019−4025

fellowship to A.J.H.G. We also thank Michael Lawson, Tivoli Olsen, Mark Richardson, and Timothy Valentic for discussions and helpful advice.

■ ABBREVIATIONS USED

CAV, caveolin-1; CAV(1−104), truncated caveolin-1; CAV-(FLV), a soluble, full length variant of caveolin-1; DLS, dynamic light scattering; ITC, isothermal calorimetry

■ REFERENCES

(1) Cohen, A. W.; Hnasko, R.; Schubert, W.; Lisanti, M. P. Role of Caveolae and Caveolins in Health and Disease. *Physiol. Rev.* **2004**, *84*, 1341−1379.
(2) Shvets, E.; Ludwig, A.; Nichols, B. J. News from the Caves: Update on the Structure and Function of Caveolae. *Curr. Opin. Cell Biol.* **2014**, *29*, 99−106.
(3) Strålfors, P. Caveolins and Caveolae, Roles in Insulin Signalling and Diabetes. *Adv. Exp. Med. Biol.* **2012**, *729*, 111−126.
(4) Zou, H.; Stoppani, E.; Volonte, D.; Galbiati, F. Caveolin-1, Cellular Senescence and Age-Related Diseases. *Mech. Ageing Dev.* **2011**, *132*, 533−542.
(5) Machado, F. S.; Rodriguez, N. E.; Adesse, D.; Garzoni, L. R.; Esper, L.; Lisanti, M. P.; Burk, R. D.; Albanese, C.; Van Doorslaer, K.; Weiss, L. M.; Nagajyothi, F.; Nosanchuk, J. D.; Wilson, M. E.; Tanowitz, H. B. Recent Developments in the Interactions between Caveolin and Pathogens. *Adv. Exp. Med. Biol.* **2012**, *729*, 65−82.
(6) Park, D. S.; Woodman, S. E.; Schubert, W.; Cohen, A. W.; Frank, P. G.; Chandra, M.; Shirani, J.; Razani, B.; Tang, B.; Jelicks, L. a; Factor, S. M.; Weiss, L. M.; Tanowitz, H. B.; Lisanti, M. P. Caveolin-1/3 Double-Knockout Mice Are Viable, but Lack Both Muscle and Non-Muscle Caveolae, and Develop a Severe Cardiomyopathic Phenotype. *Am. J. Pathol.* **2002**, *160*, 2207−2217.
(7) Lee, H.; Park, D. S.; Razani, B.; Russell, R. G.; Pestell, R. G.; Lisanti, M. P. Caveolin-1 Mutations (P132L and Null) and the Pathogenesis of Breast Cancer: Caveolin-1 (P132L) Behaves in a Dominant-Negative Manner and Caveolin-1 (−/−) Null Mice Show Mammary Epithelial Cell Hyperplasia. *Am. J. Pathol.* **2002**, *161*, 1357−1369.
(8) Schlegel, A.; Lisanti, M. P. A Molecular Dissection of Caveolin-1 Membrane Attachment and Oligomerization. Two Separate Regions of the Caveolin-1 C-Terminal Domain Mediate Membrane Binding and Oligomer/oligomer Interactions in Vivo. *J. Biol. Chem.* **2000**, *275*, 21605−21617.
(9) Hailstones, D.; Sleer, L. S.; Parton, R. G.; Stanley, K. K. Regulation of Caveolin and Caveolae by Cholesterol in MDCK Cells. *J. Lipid Res.* **1998**, *39*, 369−379.
(10) Stuart, E. S.; Webley, W. C.; Norkin, L. C. Lipid rafts, Caveolae, Caveolin-1, and Entry by Chlamydiae into Host Cells. *Exp. Cell Res.* **2003**, *287*, 67−78.
(11) Lajoie, P.; Nabi, I. R. Lipid Rafts, Caveolae, and Their Endocytosis. *Int. Rev. Cell Mol. Biol.* **2010**, *282*, 135−163.
(12) Murata, M.; Peränen, J.; Schreiner, R.; Wieland, F.; Kurzchalia, T. V.; Simons, K. VIP21/caveolin Is a Cholesterol-Binding Protein. *Proc. Natl. Acad. Sci. U. S. A.* **1995**, *92*, 10339−10343.
(13) Rothberg, K. G.; Heuser, J. E.; Donzell, W. C.; Ying, Y.-S.; Glenney, J. R.; Anderson, R. G. W. Caveolin, a Protein Component of Caveolae Membrane Coats. *Cell* **1992**, *68*, 673−682.
(14) Sargiacomo, M.; Scherer, P. E.; Tang, Z.; Kübler, E.; Song, K. S.; Sanders, M. C.; Lisanti, M. P. Oligomeric Structure of Caveolin: Implications for Caveolae Membrane Organization. *Proc. Natl. Acad. Sci. U. S. A.* **1995**, *92*, 9407−9411.
(15) Harvey, R. D.; Calaghan, S. C. Caveolae Create Local Signaling Domains through Their Distinct Protein Content, Lipid Profile and Morphology. *J. Mol. Cell. Cardiol.* **2012**, *52*, 366−375.
(16) Liu, P.; Rudick, M.; Anderson, R. G. Multiple Functions of Caveolin-1. *J. Biol. Chem.* **2002**, *277*, 41295−41298.
(17) Hovanessian, A. G.; Briand, J. P.; Said, E. A.; Svab, J.; Ferris, S.; Dali, H.; Muller, S.; Desgranges, C.; Krust, B. The Caveolin-1 Binding Domain of HIV-1 Glycoprotein gp41 Is an Efficient B Cell Epitope Vaccine Candidate against Virus Infection. *Immunity* **2004**, *21*, 617−627.
(18) Sinha, B.; Köster, D.; Ruez, R.; Gonnord, P.; Bastiani, M.; Abankwa, D.; Stan, R. V.; Butler-Browne, G.; Vedie, B.; Johannes, L.; Morone, N.; Parton, R. G.; Raposo, G.; Sens, P.; Lamaze, C.; Nassoy, P. Cells Respond to Mechanical Stress by Rapid Disassembly of Caveolae. *Cell* **2011**, *144*, 402−413.
(19) Nassoy, P.; Lamaze, C. Stressing Caveolae New Role in Cell Mechanics. *Trends Cell Biol.* **2012**, *22*, 381−389.
(20) Majumdar, S.; Hajduczki, A.; Vithayathil, R.; Olsen, T. J.; Spitler, R. M.; Mendez, A. S.; Thompson, T. D.; Weiss, G. A. In Vitro Evolution of Ligands to the Membrane Protein Caveolin. *J. Am. Chem. Soc.* **2011**, *133*, 9855−9862.
(21) Champagne, K.; Shishido, A.; Root, M. J. Interactions of HIV-1 Inhibitory Peptide T20 with the gp41 N-HR Coiled Coil. *J. Biol. Chem.* **2009**, *284*, 3619−3627.
(22) Ashkenazi, A.; Wexler-Cohen, Y.; Shai, Y. Multifaceted Action of Fuzeon as Virus−cell Membrane Fusion Inhibitor. *Biochim. Biophys. Acta, Biomembr.* **2011**, *1808*, 2352−2358.
(23) Frank, R. Spot-Synthesis: An Easy Technique for the Positionally Addressable, Parallel Chemical Synthesis on a Membrane Support. *Tetrahedron* **1992**, *48*, 9217−9232.
(24) Weiser, A.; Or-Guil, M.; Tapia, V.; Leichsenring, A.; Schuchhardt, J.; Frömmel, C.; Volkmer-Engert, R. SPOT Synthesis: Reliability of Array-based Measurement of Peptide Binding Affinity. *Anal. Biochem.* **2005**, *342*, 300−300.
(25) Kramer, A.; Reineke, U.; Dong, L.; Hoffmann, B.; Hoffmüller, U.; Winkler, D.; Volkmer-Engert, R.; Schneider-Mergener, J. Spot Synthesis: Observations and Optimizations. *J. Pept. Res.* **1999**, *54*, 319−327.
(26) Ritchie, T. J.; Macdonald, S. J. The Impact of Aromatic Ring Count on Compound Developability - Are Too Many Aromatic Rings a Liability in Drug Design? *Drug Discovery Today* **2009**, *14*, 1011−1020.
(27) Peptide library design tools. http://www.genscript.com/peptide_screening_tools.html (accessed Sep 12, 2012).
(28) Anumula, K. R.; Schulz, R. P.; Back, N. Fluorescent (Mantyl) Tag for Peptides: Its Application in Subpicomole Determination of Kinins. *Peptides* **1992**, *13*, 663−669.
(29) Pollard, T. D. A Guide to Simple and Informative Binding Assays. *Mol. Biol. Cell* **2010**, *21*, 4061−4067.
(30) Weiss, J. N. The Hill Equation Revisited: Uses and Misuses. *FASEB J.* **1997**, *11*, 835−841.
(31) Levin, A. M.; Coroneus, J. G.; Cocco, M. J.; Weiss, G. A. Exploring the Interaction between the Protein Kinase A Catalytic Subunit and Caveolin-1 Scaffolding Domain with Shotgun Scanning, Oligomer Complementation, NMR, and Docking. *Protein Sci.* **2006**, *15*, 478−486.
(32) Couet, J.; Li, S.; Okamoto, T.; Ikezu, T.; Lisanti, M. P. Identification of Peptide and Protein Ligands for the Caveolin-Scaffolding Domain. *J. Biol. Chem.* **1997**, *272*, 6525−6533.
(33) Byrne, D. P.; Dart, C.; Rigden, D. J. Evaluating Caveolin Interactions: Do Proteins Interact with the Caveolin Scaffolding Domain through a Widespread Aromatic Residue-Rich Motif? *PLoS One* **2012**, *7*, e44879.
(34) Levin, A. M.; Murase, K.; Jackson, P. J.; Flinspach, M. L.; Poulos, T. L.; Weiss, G. A. Double Barrel Shotgun Scanning of the Caveolin-1 Scaffolding Domain. *ACS Chem. Biol.* **2007**, *2*, 493−500.
(35) Shaltiel-Karyo, R.; Frenkel-Pinter, M.; Egoz-Matia, N.; Frydman-Marom, A.; Shalev, D. E.; Segal, D.; Gazit, E. Inhibiting α-Synuclein Oligomerization by Stable Cell-Penetrating β-Synuclein Fragments Recovers Phenotype of Parkinson's Disease Model Flies. *PLoS One* **2010**, *5*, e13863.
(36) Saludes, J. P.; Morton, L. A.; Ghosh, N.; Beninson, L. A.; Chapman, E. R.; Fleshner, M.; Yin, H. Detection of Highly Curved Membrane Surfaces Using a Cyclic Peptide Derived from Synaptotagmin-I. *ACS Chem. Biol.* **2012**, *7*, 1629−1635.

DOI: 10.1021/acs.jmedchem.5b01536
J. Med. Chem. 2016, 59, 4019−4025

(37) Hilpert, K.; Winkler, D. F.; Hancock, R. E. Peptide Arrays on Cellulose Support: SPOT Synthesis, a Time and Cost Efficient Method for Synthesis of Large Numbers of Peptides in a Parallel and Addressable Fashion. *Nat. Protoc.* **2007**, *2*, 1333−1349.

DOI: 10.1021/acs.jmedchem.5b01536
J. Med. Chem. 2016, 59, 4019−4025